Catalyzing urea hydrolysis using two-step microbial-induced carbonate precipitation for copper immobilization: Perspective of pH regulation

Zhong-Fei Xue[1,2], Wen-Chieh Cheng[1,2]*, Lin Wang[1,2] and Yi-Xin Xie[1,2]

[1]School of Civil Engineering, Xi'an University of Architecture and Technology, Xi'an, China, [2]Shaanxi Key Laboratory of Geotechnical and Underground Space Engineering (XAUAT), Xi'an, China

Microbial induced carbonate precipitation (MICP) has recently applied to immobilize heavy metals toward preventing their threats to public health and sustainable development of surrounding environments. However, for copper metallurgy activities higher copper ion concentrations cause the ureolytic bacteria to lose their activity, leading to some difficulty in forming carbonate precipitation for copper immobilization (referred to also as "biomineralization"). A series test tube experiments were conducted in the present work to investigate the effects of bacterial inoculation and pH conditions on the copper immobilization efficiency. The numerical simulations mainly aimed to compare with the experimental results to verify its applicability. The copper immobilization efficiency was attained through azurite precipitation under pH in a 4−6 range, while due to Cu^{2+} migration and diffusion, it reduced to zero under pH below 4. In case pH fell within a 7−9 range, the immobilization efficiency was attained via malachite precipitation. The copper-ammonia complexes formation reduced the immobilization efficiency to zero. The reductions were attributed either to the low degree of urea hydrolysis or to inappropriate pH conditions. The findings shed light on the necessity of securing the urease activity and modifying pH conditions using the two-step biomineralization approach while applying the MICP technology to remedy copper-rich water bodies.
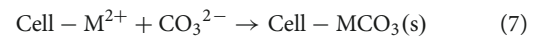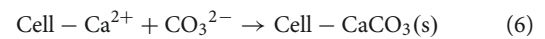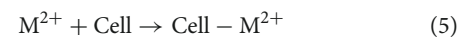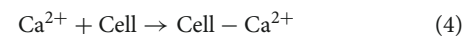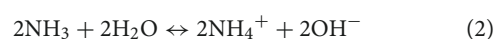
KEYWORDS

microbial-induced carbonate precipitation, ureolytic bacteria, copper metal, two-step biomineralization, copper-ammonia complex

Introduction

Copper (Cu) is an indispensable trace element for human health, plant and animal growth, and it has an activating effect on some key enzymes in cellular metabolism (Facchin et al., 2013). However, it can impose serious threats to organisms if the concentration exceeds the legal limit (Elalfy et al., 2021; Guo et al., 2021). Most of the copper in nature exists as compounds (i.e., copper minerals), and in China, the development of copper mining, smelting, and processing has raised the potential of their migration and diffusion in surrounding environments (Bai et al., 2021b,c; Hu et al., 2021a, 2022a,b; Wang et al., 2022b; Xue et al., 2021; Yu et al., 2021). Nowadays there are various physical and chemical measures available for remedying copper-rich water bodies. However, these methods are time-consuming, costly, and not environmental-friendly (Qdais and Moussa, 2004; Wei et al., 2005; Fu and Wang, 2011; You et al., 2018; Chen et al., 2022a,b; Li et al., 2022; Wang et al., 2022a). In recent years, the microbial-induced carbonate precipitation (MICP) technology has attracted extensive attention as an alternative to traditional measures (Achal et al., 2012a; Chen and Achal, 2019; Ye et al., 2021; Xue et al., 2022a,b).

The MICP technology can precipitate carbonates between soil particles and has been widely applied to calcareous sand reinforcement (Jiang et al., 2019; Lai et al., 2020; Rahman et al., 2020; Zhang et al., 2020; Cui et al., 2021; Xiao et al., 2021; Yang et al., 2022), while studies on the remediation of heavy metals using the MICP technology are markedly limited (Kang et al., 2015; Li et al., 2021; Wang et al., 2022e,f). The principle of the MICP technology is to catalyze urea hydrolysis through secreting the urease using the ureolytic bacteria, discharging hydroxide and ammonium ions (see Eqs. 1–3) and subsequently yielding carbonates. Heavy metal ions and calcium ions could co-precipitate with bacteria as nucleation sites in the biomineralization process (see Eqs. 4–7) (Li et al., 2013). As a result, the "net" effect of such a reaction corresponds to an increase in surrounding pH (Schwantes-Cezario et al., 2017; Cui et al., 2022). The use of carbonates aims to capsulize heavy metal ions by forming carbonate precipitation (termed immobilization of heavy metals hereafter), preventing their migration and diffusion (Achal et al., 2011; Achal et al., 2012b; Jiang and Soga, 2019; Chen and Achal, 2019; Schwantes-Cezario et al., 2020; Liu et al., 2021; Mujah et al., 2021; Zeng et al., 2021). Ali et al. (2022) reported that strain *B. diminuta* isolated from soil could immobilize Cd^{2+} and Zn^{2+} in solution by co-precipitation. In addition, extracellular polymers (EPS) secreted by bacteria can provide nucleation sites and promote bacteria to immobilize heavy metal ions in solution (Chen et al., 2016; Casas et al., 2020; Qiao et al., 2021; Kim et al., 2021).

$$CO(NH_2)_2 + H_2O \rightarrow 2NH_3 + CO_2 \quad (1)$$

$$2NH_3 + 2H_2O \leftrightarrow 2NH_4^+ + 2OH^- \quad (2)$$

$$CO_2 + 2OH^- \leftrightarrow HCO_3^- + OH^- \leftrightarrow CO_3^{2-} + H_2O \quad (3)$$

$$Ca^{2+} + Cell \rightarrow Cell - Ca^{2+} \quad (4)$$

$$M^{2+} + Cell \rightarrow Cell - M^{2+} \quad (5)$$

$$Cell - Ca^{2+} + CO_3^{2-} \rightarrow Cell - CaCO_3(s) \quad (6)$$

$$Cell - M^{2+} + CO_3^{2-} \rightarrow Cell - MCO_3(s) \quad (7)$$

Recent studies indicated that the copper immobilization efficiency generally maintains at low levels compared to other heavy metals (Achal et al., 2011; Li et al., 2013; Mugwar and Harbottle, 2016; Bai et al., 2019, 2021a; Hu et al., 2021b; Wang et al., 2022c,d). It is due to the fact that copper ions bind to the functional groups of the urease, and as a result, its spatial structure is badly modified causing its denaturation and inactivation (Krajewska, 2008; Seplveda et al., 2021). Among all the positive divalent heavy metals, copper has the highest toxicity on the urease activity except mercury, and securing the urease activity against copper metal is deemed a challenging task while introducing the MICP technology (Zaborska et al., 2004; Jiang et al., 2019). Increasing the initial urea concentration may improve the resistance of the urease against copper metal. However, the higher the urea concentration, the higher the surrounding pH, and the higher the potential of forming complexes unfavorable for the immobilization of copper metal (Ferris et al., 2004; Torres-Aravena et al., 2018; Duarte-Nass et al., 2020; Liu et al., 2020; Seplveda et al., 2021; Tarach et al., 2021; Chen et al., 2022a,c; Xue et al., 2022c).

Conducting a closer look to the literature on the biomineralization, however, reveals a number of gaps and shortcomings. To this end, the present work proposes a two-step biomineralization approach; the first step allows the ureolytic bacteria hydrolyze urea to discharge the amount of carbonate and hydroxyl ions necessary for forming carbonates in the second step. The second step mainly aims to use the ureolytic bacteria as nucleation sites to precipitate carbonate, capsulizing copper metal (Torres-Aravena et al., 2018; Duarte-Nass et al., 2020). Prior to the second step where the urease is inoculated to the medium containing copper metal, the amount of carbonate and ammonia ions necessary for forming carbonates in the second step is already yielded in the first step, mitigating the effect of Cu^{2+} toxicity. In addition, different inoculation proportions may consider in the second step to modify the surrounding pH, thus preventing the formation of complexes unfavorable for securing the copper immobilization efficiency. The objectives of this study are: (1) To conduct test tube experiments to investigate the effects of bacterial inoculation and pH surrounding conditions, (2) to highlight the necessity of modifying pH and distinguish the speciation of precipitation against different pH ranges using the numerical simulations, and (3) to propose the two-step biomineralization approach to secure the immobilization efficiency.

Materials and methods

Ureolytic bacteria culture

Sporosarcina pasteurii, a basophilic ureolytic bacterium, was used in the present work. It was activated in a sterile liquid medium, which consists of 20 g/L yeast extract, 10 g/L NH_4Cl, 20 g/L urea, 10 mg/L $MnSO_4 \cdot H_2O$, 24 mg/L $NiCl_2 \cdot 6H_2O$. The surrounding pH for the sterile liquid medium was adjusted to 8.8 using 1 M solution of NaOH. The activated ureolytic bacteria were mixed with glycerol using a ratio of 7:3 and stored at −20 °C. They were subjected to shaking culture at 30 °C and 180 rpm for 30 h. Further, the chemicals of urea, $MnSO_4 \cdot H_2O$, $NiCl_2 \cdot 6H_2O$, NaOH, and $Cu(NO_3)_2 \cdot 3H_2O$ were diluted to given concentrations, respectively, and applied to the subsequent test tube experiments.

Urease activity measurement

The urease activity (termed UA hereafter) under different bacterial inoculation proportions was measured in Cu^{2+} contained 0.5 M urea solution, which aims to evaluate the effect of Cu^{2+} toxicity on the ureolytic bacteria and urease activity. The concentration of Cu^{2+} and the bacterial inoculation proportion were 5, 10, and 20 mM, and 1:9, 1:3, and 1:1, respectively.

pH, EC (electric conductivity), and UA, while catalyzing urea hydrolysis, were measured using a benchtop pH meter (Hanna Instruments Inc. HI2003) and a benchtop conductivity meter (Hanna Instruments Inc. HI2314), respectively. UA was measured on a basis of the ureolysis rate, as recommended by Whiffin et al. (2007); 2 mL final reaction solution is mixed with 18 mL 1.11 M urea, and EC is measured at 0 min and 5 min after the mixing. UA can be evaluated using the equation below:

$$UA = \frac{EC_5 - EC_0}{5} \times 10 \times 1.11 (\text{mM Urea min}^{-1}) \quad (8)$$

where EC_0 and EC_5 are electrical conductivity at 0 and 5 min, respectively. NH_4^+ concentration of the final reaction solution is measured at 0, 24 and 48 h, respectively, and the method for measuring NH_4^+ concentration corresponds to the

TABLE 2 Scheme applied to the test tube experiments.

Parameters applied to the first step	Parameters applied to the second step	Concentration of $Cu(NO_3)_2$ (mM)
Urea at 333 mM NH_4Cl at 187 mM	1:9	20, 40, 60
	1:3	20, 40, 60
	1:1	0–50

modified Nessler method (Whiffin et al., 2007). There were three replicates for each test set.

Numerical simulations

To evaluate the effect of Cu^{2+} concentration and pH on the speciation of precipitation and copper immobilization efficiency, the biomineralization process was reproduced using the Visual MINTEQ software package, although the process of urea hydrolysis has been neglected. The initial concentration for NH_4^+ and CO_3^{2-} was calculated in accordance with the bacterial inoculation proportion. Table 1 summarize the parameters applied to the numerical simulations.

Test tube experiments

This part aims to elaborate more about the details applied to the test tube experiments. First, a $Cu(NO_3)_2$ solution at concentrations varying in a 0–60 mM range was prepared, while the ureolytic bacteria were cultivated with yeast extract and ammonia nitrogen, during which time urea at 333 mM was also added to the culture medium. Second, the urea hydrolysis proceeded with the bacterial inoculation proportions of 1:9, 1:3, and 1:1, respectively, for 48 consecutive hours. The aforesaid two-step biomineralization approach is the first proposed by the authors and primarily aims not only to discharge NH_4^+ and OH^- preventing not only the effect of Cu^{2+} toxicity but the formation of complexes unfavorable for securing the copper immobilization efficiency. NH_4^+ and Cu^{2+} concentrations were measured at 0, 24, and 48 h, respectively. An atomic

TABLE 1 Parameters applied to the numerical simulations of the copper immobilization efficiency against $Cu(NO_3)_2$ concentration and pH considering bacterial inoculation proportions of 1:9, 1:3, 1:1, and 3:1, respectively.

Bacterial inoculation proportion	Ion concentration (mM)					pH
	Cu^{2+}	NO_3^-	NH_4^+	CO_3^{2-}	Cl^-	
1:9	5, 20, 40, 60, 80	10, 40, 80, 120, 160	85.3	33.3	18.7	0–13
1:3			213.25	83.25	46.75	
1:1			426.5	166.5	93.5	
3:1			639.75	249.75	140.25	

spectrophotometer (Beijing Purkinje General Instrument TAS-990) was responsible for the Cu^{2+} concentration measurements. The copper immobilization efficiency can be evaluated as follows:'

$$\text{Immobilization efficiency} = ((C_0 - C_1)/C_0) \times 100\% \quad (9)$$

where C_0 and C_1 are Cu^{2+} ions concentration before and after remediation, respectively. **Table 2** summarize the scheme applied to the test tube experiment. There were three replicates for each test set.

Results and discussion

Test tube experiments

Effect of bacterial inoculation

UA is an important indicator that determines the growth and reproduction of the ureolytic bacteria during the biomineralization process. Furthermore, the higher the UA, the higher the resistance of the ureolytic bacteria against copper metal (Song et al., 2017). Considering copper metal can significantly impede the bacteria's growth and reproduction (Zaborska et al., 2004), the degradation mechanism is summarized as copper metal binding to the functional groups of the urease and modifying its spatial structure, thus causing its denaturation and inactivation (Krajewska, 2008). Duarte-Nass et al. (2020) suggested that increasing the initial urea concentration could improve the resistance of ureolytic bacteria against Cu^{2+} toxicity. Despite that, such high initial urea concentration, however, turns the surrounding pH into alkaline environments promoting the formation of copper-ammonia complexes unfavorable for securing the copper immobilization efficiency (Liu et al., 2018; Duarte-Nass et al., 2020).

When subjected to 20 mM Cu^{2+}, UA goes into a decline for the bacterial inoculation proportion = 1:1, while for the bacterial inoculation proportions = 1:3 and 1:9, it shows a smaller change (see **Figure 1A**). UA for all the bacterial inoculation proportions reduces to approximately zero 4 h after the beginning of bacterial inoculation, indicating that the effect of Cu^{2+} toxicity depresses the growth and reproduction of the ureolytic bacteria and causes some difficulty in catalyzing urea hydrolysis. For this reason, the measurements of EC and NH_4^+ show a small change because of a small number of NH_4^+ and OH^- discharged, as depicted in **Figures 1B,C**. UA for the

FIGURE 1
(A) UA vs. treatment time relationship, **(B)** EC vs. treatment time relationship, and **(C)** NH_4^+ vs. treatment time relationship when subjected to Cu^{2+} concentration at 20 mM.

FIGURE 2
(A) UA vs. treatment time relationship, **(B)** EC vs. treatment time relationship, and **(C)** NH$_4^+$ vs. treatment time relationship when subjected to Cu^{2+} concentration at 10 mM.
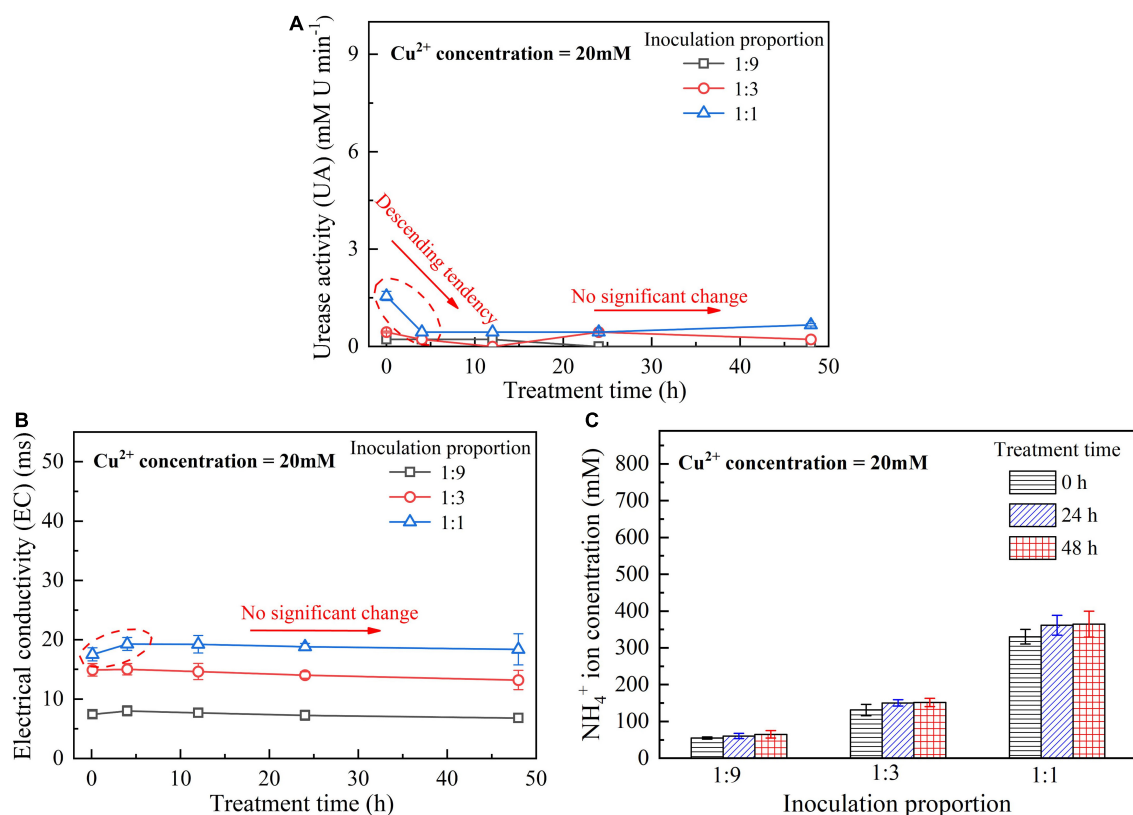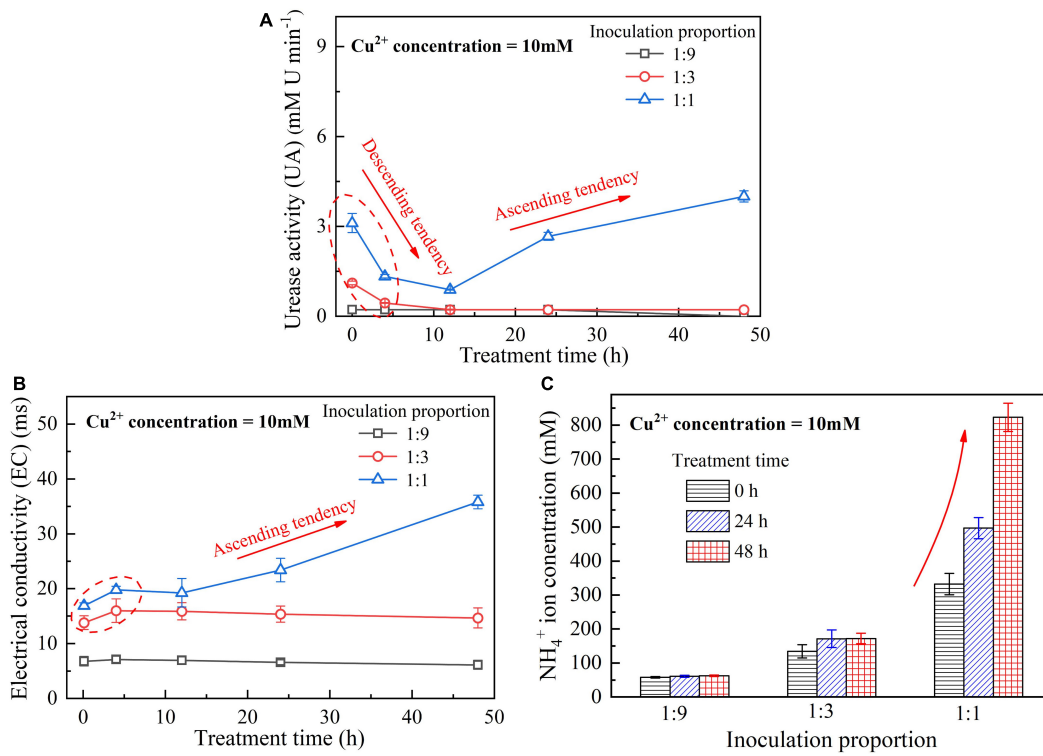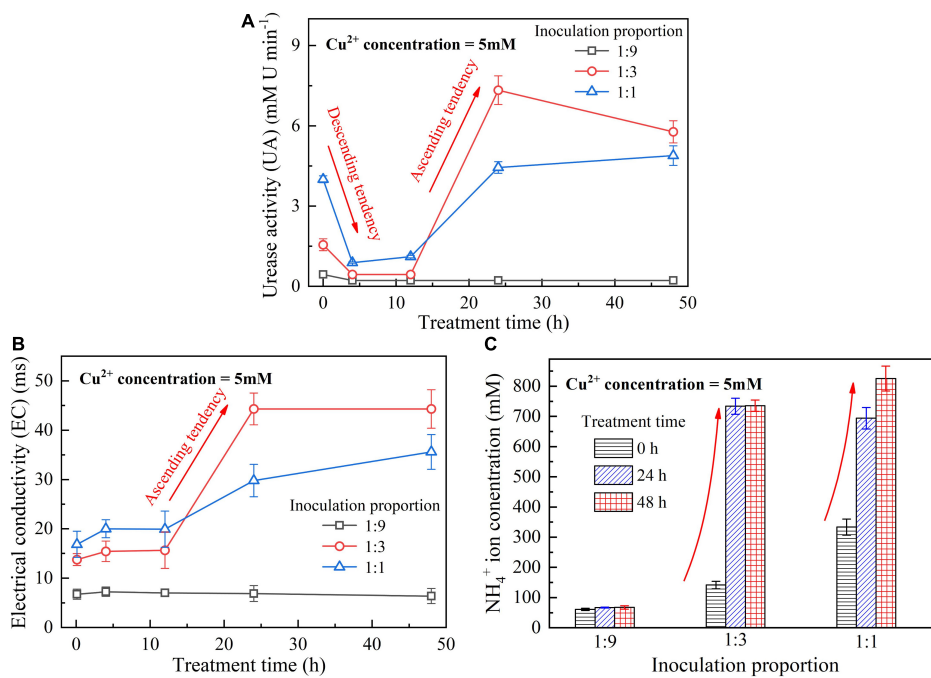

FIGURE 3
(A) UA vs. treatment time relationship, **(B)** EC vs. treatment time relationship, and **(C)** NH$_4^+$ vs. treatment time relationship when subjected to Cu^{2+} concentration at 5 mM.

FIGURE 4
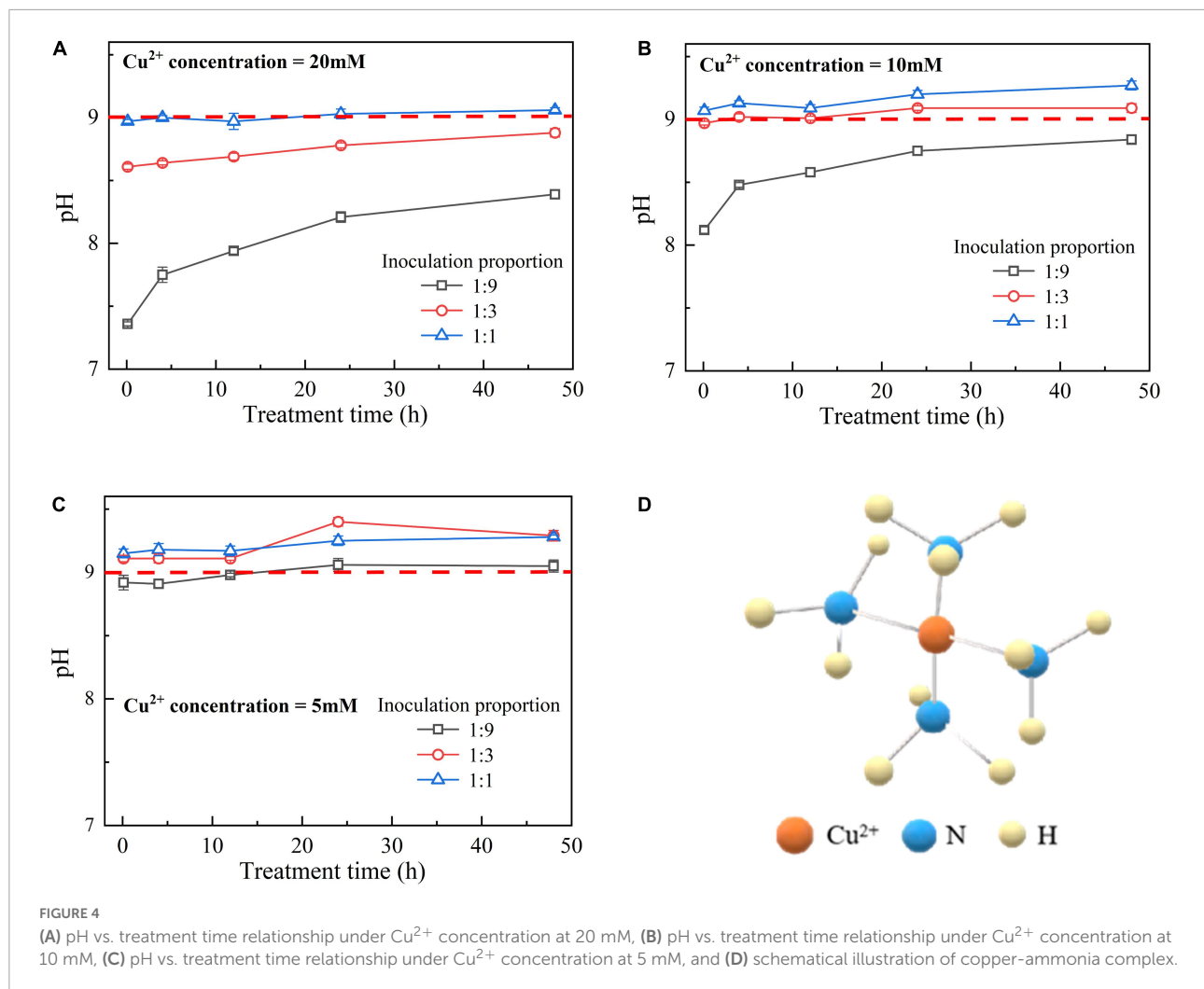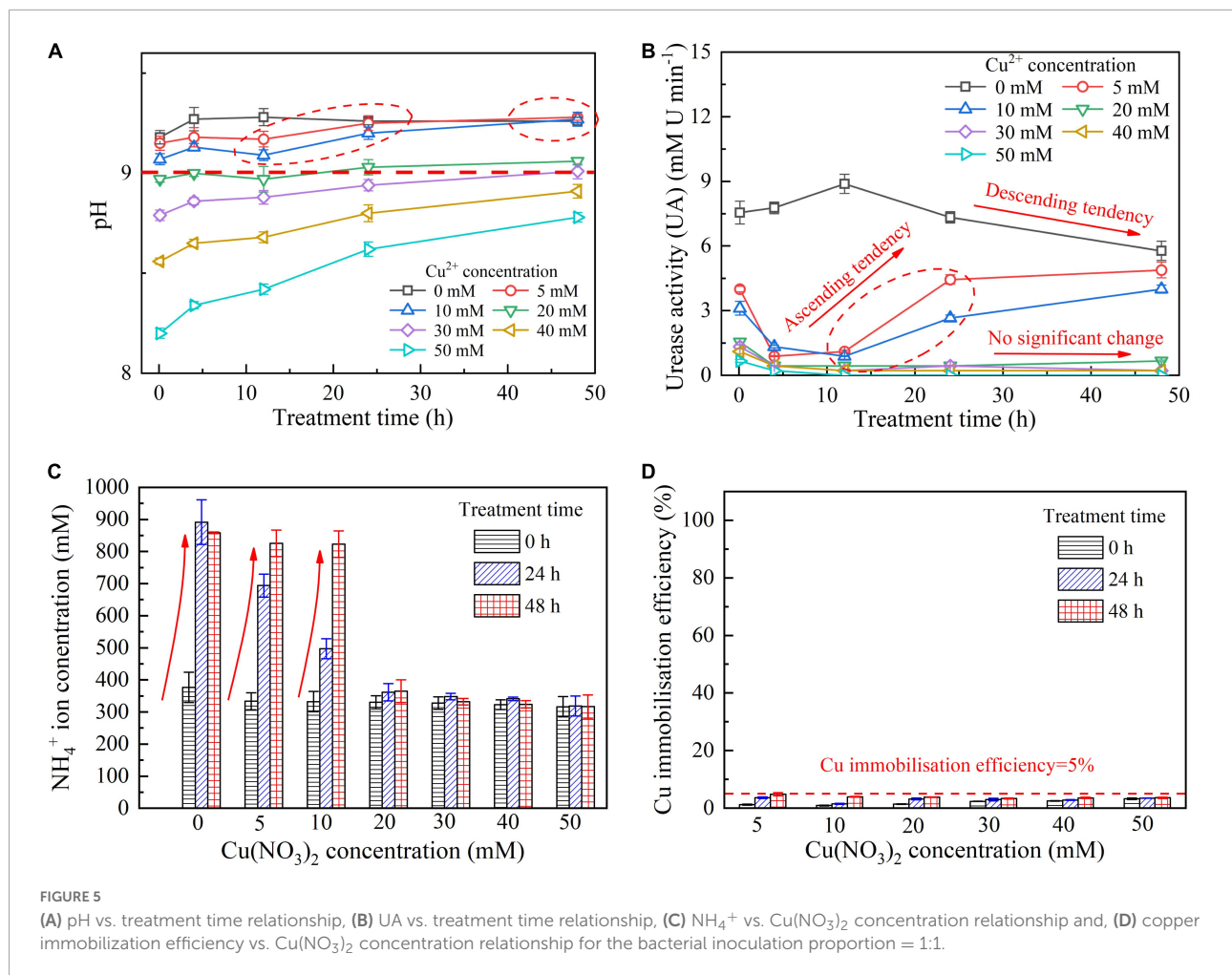(A) pH vs. treatment time relationship under Cu^{2+} concentration at 20 mM, (B) pH vs. treatment time relationship under Cu^{2+} concentration at 10 mM, (C) pH vs. treatment time relationship under Cu^{2+} concentration at 5 mM, and (D) schematical illustration of copper-ammonia complex.

bacterial inoculation proportion = 1:1 goes into a decline at the very beginning of bacterial inoculation when subjected to 10 mM Cu^{2+}, and goes up 12 h following the commencement of bacterial inoculation, as shown in Figure 2A. In contrast, UA for the other two inoculation proportions presents a negligible change all long. These results indicate that the ureolytic bacteria for the bacterial inoculation proportion = 1:1 could remain its activity when subjected to 10 mM Cu^{2+}, and for the other two inoculation proportions, the effect of Cu^{2+} toxicity depresses the growth and reproduction of the ureolytic bacteria reducing the secretion of the urease. The measurements of EC and NH_4^+ provide testimony of the above argument, as shown in Figures 2B,C. Given the inoculation proportion = 1:1, UA going up 12 h after the beginning of bacterial inoculation is attributed to the reduction in the effect of Cu^{2+} toxicity, induced by the formation of copper-ammonia complexes. In other words, the formation of copper-ammonia complexes causes an inability of depressing the growth of the ureolytic bacteria and enhances the resistance of the urease against Cu^{2+} toxicity. When subjected

to 5 mM Cu^{2+}, the behavior can also be recognized as UA going down rapidly and going up till the end of the process and becomes more distinct compared to 10 mM Cu^{2+}. UA for the inoculation proportion = 1:3 even surpasses that for the inoculation proportion = 1:1 12 h after the commencement of bacterial inoculation. The relatively higher urea concentration for the inoculation proportion = 1:3 may be considered as the main cause leading to such phenomenon. EC and NH_4^+ measurements give testimony to the argument made, as shown in Figures 3B,C.

On the whole, when subjected to 20 mM Cu^{2+}, either for higher inoculation proportions or lower inoculation proportions the majority of the ureolytic bacteria lose their activity in the first 4 h because of the effect of Cu^{2+} toxicity. For this reason, a small number of NH_4^+ and OH^- are discharged and EC, therefore, shows a small increase. The effect of Cu^{2+} toxicity badly depresses the growth and reproduction of the ureolytic bacteria for the subsequent 8 h. The ureolytic bacteria that remain active 12 h after the
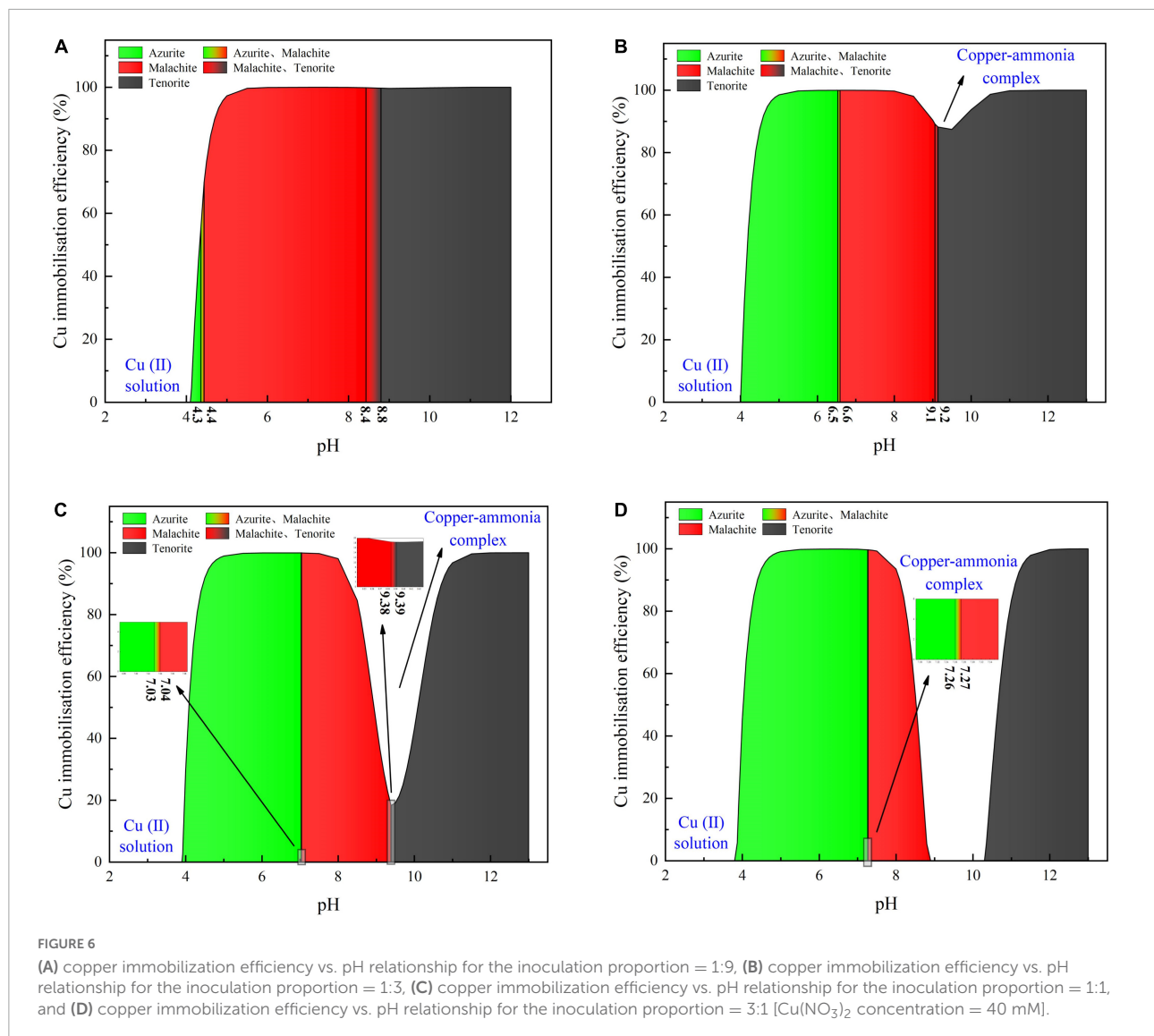
FIGURE 5
(A) pH vs. treatment time relationship, **(B)** UA vs. treatment time relationship, **(C)** NH_4^+ vs. $Cu(NO_3)_2$ concentration relationship and, **(D)** copper immobilization efficiency vs. $Cu(NO_3)_2$ concentration relationship for the bacterial inoculation proportion = 1:1.

commencement of bacterial inoculation begin showing their resistance against Cu^{2+} toxicity. The formation of copper-ammonia complexes reduces the effect of Cu^{2+} toxicity on the ureolytic bacteria and UA. This phenomenon becomes more pronounced when subjected to lower Cu^{2+} concentrations and higher bacterial inoculation proportions (e.g., 1:3 and 1:1). When subjected to 10 mM Cu^{2+}, the ureolytic bacteria remain active only when the bacterial inoculation proportion is raised to 1:1, whereas the ureolytic bacteria, when subjected to 5 mM Cu^{2+}, remain active even when the inoculation proportion is reduced to 1:3. These results lead us to summarize that although higher inoculation proportions can improve the resistance of the ureolytic bacteria against Cu^{2+} toxicity and promote the secretion of the urease, their use is accompanied by discharging more OH^- throughout the biomineralization process, turning surrounding environments into alkaline conditions and promoting the copper-ammonia complexes formation. The copper-ammonia complexes largely raise the potential of Cu^{2+} migration and diffusion, causing an inability of securing the copper immobilization efficiency. As indicated by **Figure 3C**, an improvement in EC and

NH_4^+ may cause misleading interferences concerning the use of high inoculation proportion of 1:1 for improving the copper immobilization efficiency. Therefore, it is argued that higher inoculation proportions pave the way to secure copper immobilization efficiency. In addition to UA, particular attention to the surrounding pH conditions should also be given, preventing a reduction in the copper immobilization efficiency by the copper-ammonia complexes formation.

Effect of surrounding pH conditions

The temporal relationships of pH against the bacterial inoculation proportion = 1:9, 1:3, and 1:1 when subjected to 20, 10, and 5 mM Cu^{2+} are shown in **Figures 4A–C**, respectively. The results from the previous section indicate that when subjected to 10 mM Cu^{2+}, the ureolytic bacteria remaining active is present only when the inoculation proportion is raised to 1:1, while the bacteria that remain active, when subjected to 5 mM Cu^{2+}, presents even when the inoculation proportion is as low as 1:3. The value of surrounding pH corresponding to the these results, however, exceeds 9 (Duarte-Nass et al., 2020). As discussed, the ureolytic bacteria can be characterized

FIGURE 6
(A) copper immobilization efficiency vs. pH relationship for the inoculation proportion = 1:9, **(B)** copper immobilization efficiency vs. pH relationship for the inoculation proportion = 1:3, **(C)** copper immobilization efficiency vs. pH relationship for the inoculation proportion = 1:1, and **(D)** copper immobilization efficiency vs. pH relationship for the inoculation proportion = 3:1 [$Cu(NO_3)_2$ concentration = 40 mM].

as UA going down in the first 4 h after the commencement of bacterial inoculation, and UA going up since after 12 h (see **Figures 2A**, **3A**). The bacteria that remain active 12 h after the commencement of bacterial inoculation can reproduce and catalyze urea hydrolysis, discharging NH_4^+ and OH^-. This is deemed as the main cause leading to the value of pH in excess of 9.

pH below 9 is attained using 20–50 mM Cu^{2+} where the effect of Cu^{2+} toxicity can depress the growth and reproduction of the ureolytic bacteria (see **Figures 5A,B**). The ureolytic bacteria remain active when subjected to 0–10 mM Cu^{2+}, discharging NH_4^+ throughout the biomineralization process (see **Figure 5C**). It is worth to note that the copper immobilization efficiency could be as low as 5% under the inoculation proportion being 1:1, and such low copper immobilization efficiency still holds true when Cu^{2+}

concentration decreases to 5 mM (see **Figure 5D**). These results conflict with our consensus that lower Cu^{2+} concentrations can ease the effect of Cu^{2+} toxicity on the ureolytic bacteria and promote the secretion of the urease by the ureolytic bacteria, thus improving the degree of urea hydrolysis and subsequently the copper immobilization efficiency. There are two underlying mechanisms revealed by the present work. Although the ureolytic bacteria remain active when subjected to 0–10 mM Cu^{2+}, the highest inoculation proportion of 1:1 not only eases the effect of Cu^{2+} toxicity on the ureolytic bacteria and UA but turns the surrounding pH into alkaline conditions (pH > 9), promoting the formation of copper-ammonia complexes. The copper-ammonia complexes raise the potential of Cu^{2+} migration and diffusion and reduce the copper immobilization efficiency to as low as 5%. Furthermore, despite pH below 9 and no copper-ammonia complex formation, the
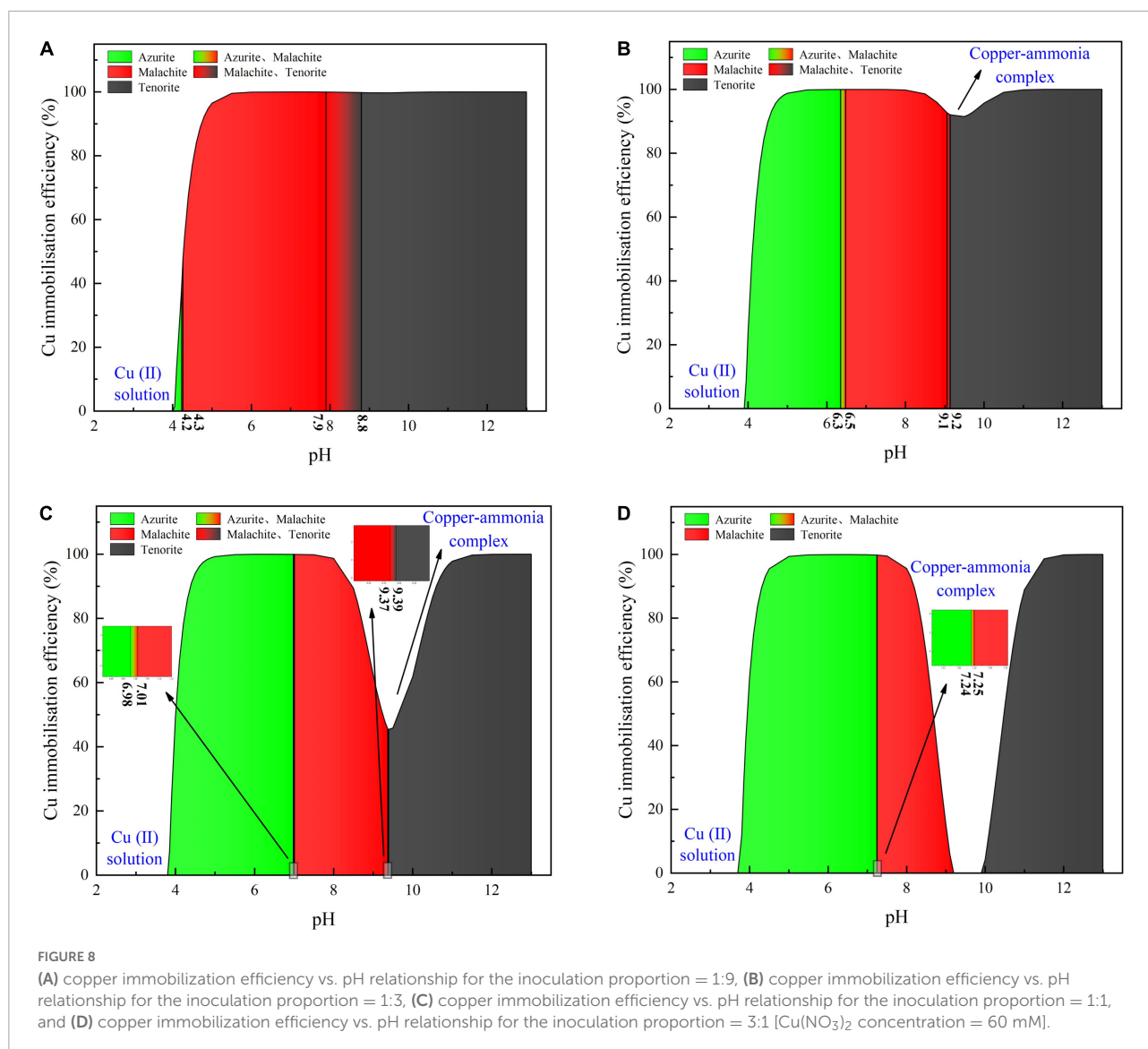
(A) copper immobilization efficiency vs. pH relationship for the inoculation proportion = 1:9, **(B)** copper immobilization efficiency vs. pH relationship for the inoculation proportion = 1:3, **(C)** copper immobilization efficiency vs. pH relationship for the inoculation proportion = 1:1, and **(D)** copper immobilization efficiency vs. pH relationship for the inoculation proportion = 3:1 [Cu(NO$_3$)$_2$ concentration = 20 mM].

effect of Cu^{2+} toxicity badly depresses the ureolytic bacteria and UA when subjected to a range of 20–50 mM Cu^{2+}, reducing the degree of urea hydrolysis. The lower the degree of urea hydrolysis, the lesser the carbonate precipitated, and the lower the copper immobilization efficiency. The reduction in the degree of urea hydrolysis reduces the copper immobilization efficiency to approximately 5%.

Numerical simulations

Considering harsh pH conditions and the precipitation speciation have been neglected in the test tube experiments, they are interpreted a step further using a series of numerical simulations. Given 40 mM Cu(NO$_3$)$_2$, the relationships of the copper immobilization efficiency vs. the surrounding pH against the inoculation proportions of 1:9, 1:3, 1:1, and 3:1 are

shown in **Figure 6**. Under the inoculation proportion = 1:9, there are three speciations of carbonate precipitation, including azurite [(Cu$_3$(OH)$_2$(CO$_3$)$_2$)], malachite [Cu$_2$(OH)$_2$CO$_3$], and tenorite (CuO), when pH remains above 4 (see **Figure 6A**). The copper immobilization efficiency increases notably when pH is increased from 4.0 to 4.5. It reaches approximately 100% when pH falls within a 5–12 range, with the exception of pH surrounding 9 where a reduction in the copper immobilization efficiency occurs. When pH is below 4, Cu^{2+} are present in a free state and no carbonate precipitation is found, reducing the copper immobilization efficiency to zero. The aforesaid three speciations of carbonate precipitation are also present under the inoculation proportion = 1:3 (see **Figure 6B**). Similarly, Cu^{2+} are present in a free state when pH remains below 4. Except pH surrounding 9, the copper immobilization efficiency reaches nearly 100% as pH falls within a 5–12 range. Such reduction in the copper immobilization efficiency under the

FIGURE 8

(A) copper immobilization efficiency vs. pH relationship for the inoculation proportion = 1:9, **(B)** copper immobilization efficiency vs. pH relationship for the inoculation proportion = 1:3, **(C)** copper immobilization efficiency vs. pH relationship for the inoculation proportion = 1:1, and **(D)** copper immobilization efficiency vs. pH relationship for the inoculation proportion = 3:1 [Cu(NO$_3$)$_2$ concentration = 60 mM].

inoculation proportion = 1:1 and 3:1, respectively, is also noted (see **Figures 6C,D**). It is also present when subjected to 20 mM and 60 mM Cu(NO$_3$)$_2$, respectively (see **Figures 7**, **8**). In this situation (pH approximately 9) precipitation even disappears under the inoculation proportion = 3:1. Taking a close look at the variations of the copper immobilization efficiency shown in **Figures 6–8**, higher Cu^{2+} concentrations narrow pH ranges that are associated with the formation of copper-ammonia complexes. For example, pH corresponding to the formation of copper-ammonia complexes is narrowed from 8.2 to 10.2 range when subjected to 20 mM Cu^{2+} to 8.6–10 range when subjected to 60 mM Cu^{2+}. In other words, there is a higher possibility for the copper-ammonia complexes to form when subjected to lower Cu^{2+} concentrations. These phenomena are due to the fact that lower Cu^{2+} concentrations in fact turn surrounding environments into alkaline conditions favorable

for forming the copper-ammonia complexes. In contrast, higher Cu^{2+} concentrations provide acidic environments.

In acidic environments, the hydrolysis of CO$_3$$^{2-}$ is going forward and ammonia is present in NH$_4$$^+$ form. Considering HCO$_3$$^-$ and H$_2$CO$_3$ as well as NH$_4$$^+$ are not going to react with Cu^{2+}, the majority of Cu^{2+} is present in a free state and the remaining is biomineralized with CO$_3$$^{2-}$, thereby forming azurite precipitation (see **Figures 6–8**). Under pH below 4, Cu^{2+} in a free state raises its migration and diffusion potential and is deemed as the main contributor to the reduction in the copper immobilization efficiency. In short, under pH in a 4–6 range (in most cases), the copper immobilization efficiency is attained through azurite precipitation. The copper immobilization efficiency drops sharply to zero under pH below 4 due to Cu^{2+} migration and diffusion. In contrast, the hydrolysis of CO$_3$$^{2-}$ is going backward in alkaline environments, and ammonia is, in
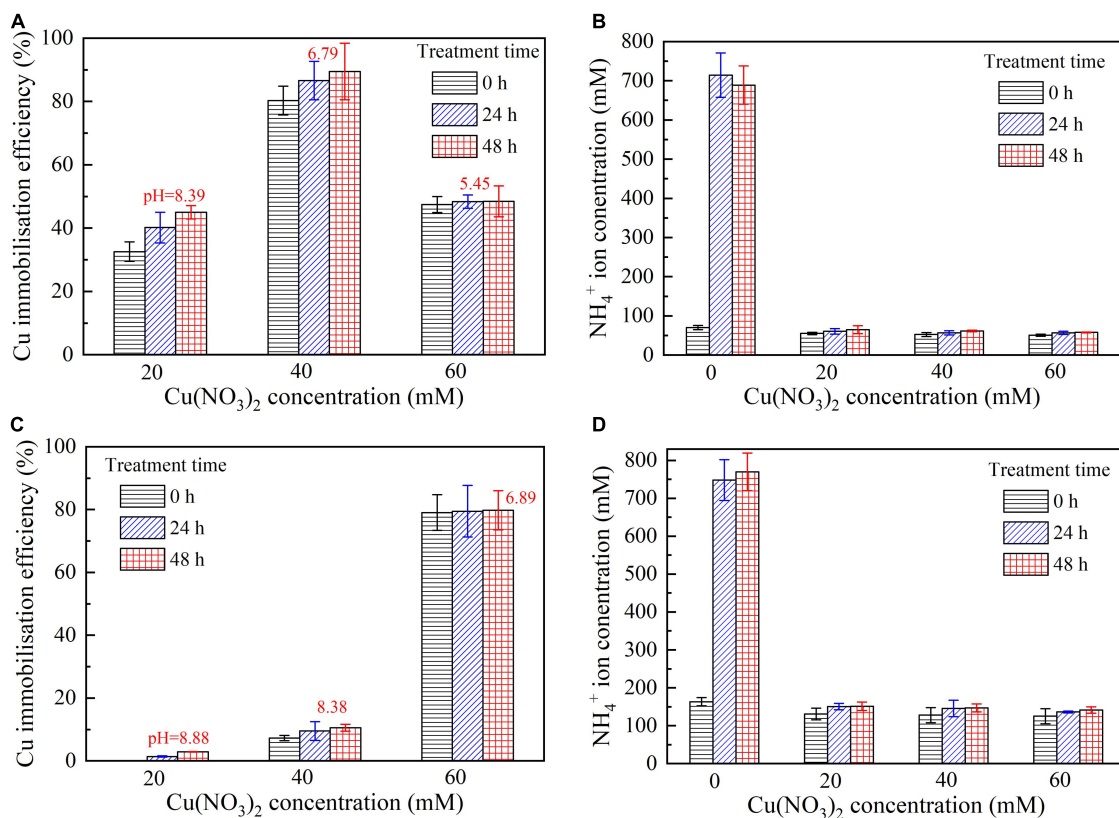
FIGURE 9
(A) copper immobilization efficiency vs. $Cu(NO_3)_2$ concentration relationship and **(B)** NH_4^+ concentration vs. $Cu(NO_3)_2$ concentration relationship for the inoculation proportion = 1:9; **(C)** copper immobilization efficiency vs. $Cu(NO_3)_2$ concentration relationship and **(D)** NH4 + concentration vs. $Cu(NO_3)_2$ concentration relationship for the inoculation proportion = 1:3.

turn, present in NH_3 form. NH_3 is going to react with Cu^{2+}, forming the copper-ammonia complexes. The remaining is going to precipitate with CO_3^{2-} to form malachite precipitation (see **Figures 6–8**). It is noteworthy that tenorite is precipitated under pH above 10, corresponding to a copper immobilization efficiency of approximately 100%. Notwithstanding that, its chemical and thermodynamic properties are not as good as the other two carbonates (i.e., azurite and malachite) because it dissolves under harsh pH and temperature conditions, causing an inability of preventing Cu^{2+} migration and diffusion. To summarize, under pH surrounding 9, the copper-ammonia complexes notably reduce the copper immobilization efficiency to zero by promoting Cu^{2+} migration and diffusion. In case pH falls within a 7–9 range (in most cases), the copper immobilization efficiency is attained through malachite precipitation.

Copper immobilization efficiency

This part aims not only to verify the applicability of the numerical simulations applied to the present work but to

investigate further the effect of Cu^{2+} concentration on the immobilization efficiency under a given pH value (Mugwar and Harbottle, 2016). It can be observed that for the inoculation proportion = 1:9, the copper immobilization efficiency being approximately 90% is the highest under $Cu(NO_3)_2$ concentration at 40 mM, corresponding to pH = 6.79 (see **Figures 9B,D**). Further, the copper immobilization efficiency approximately 45% is the lowest when subjected to $Cu(NO_3)_2$ concentration at 20 mM, which corresponds to pH = 8.39. These results are in line with the simulated results, thereby verifying the applicability of the numerical simulations (see **Figures 6–8**). The reductions in the copper immobilization efficiencies, when subjected to $Cu(NO_3)_2$ = 20 mM and 60 mM, appear to be attributed to the effect of pH conditions. Although the majority of the ureolytic bacteria lose their activity in the second step of the two-step biomineralization, the discharge of OH^- (relevant to bacterial inoculation proportion) in the first step determine not only pH conditions but also the speciation of carbonate precipitation. pH = 8.88, induced by the inoculation proportion = 1:3, gives alkaline environments when subjected to 20 mM $Cu(NO_3)_2$ and promotes the formation of copper-ammonia complexes,
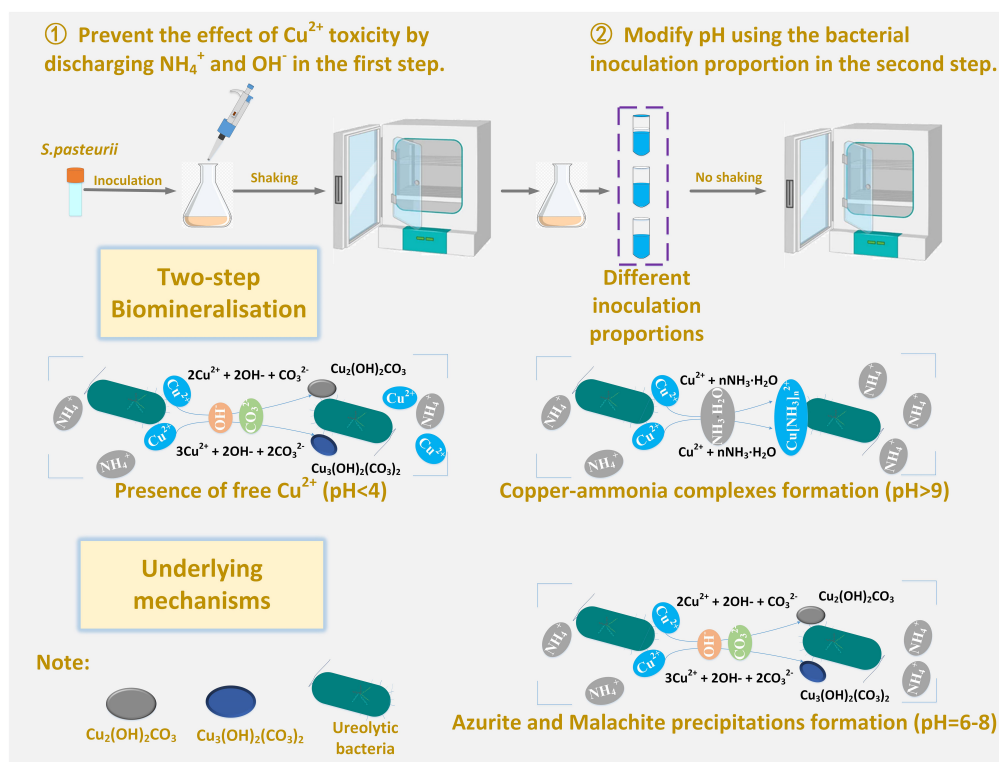
FIGURE 10

Schematic illustration of the underlying mechanisms affecting the copper immobilization efficiency.

yielding the copper immobilization efficiency way below 10% (see **Figures 9C,D**). In contrast, when subjected to 60 mM $Cu(NO_3)_2$, pH = 6.89, resulting from the inoculation proportion = 1:3, gives acidic environments and then prevent the formation of copper-ammonia complexes, corresponding to the copper immobilization efficiency approximately 80%. In most cases the copper immobilization efficiency using the two-step biomineralization approach higher than 45% is much higher than that using the ordinary biomineralization approach despite a discrepancy in the bacterial inoculation proportion (see **Figure 5D**). That is to say, the two-step biomineralization approach elevates the copper immobilization efficiency and such improvement is especially pronounced when subjected to higher $Cu(NO_3)_2$ concentrations. However, the copper immobilization efficiency way below 10% under the bacterial inoculation proportion = 1:3 appears when subjected to 20 mM $Cu(NO_3)_2$. Modification concerning pH conditions may consider by reducing the inoculation proportion to 1:9 to prevent the reduction in the copper immobiliztion efficiency. To conclude, the two-step biomineralization approach prevents the effect of Cu^{2+} toxicity by discharging NH_4^+ and OH^- prior to inoculating the ureolytic bacteria to the liquid medium containing $Cu(NO_3)_2$. Discharging NH_4^+ and OH^- while cultivating the ureolytic bacteria is deemed as the first step (see **Figure 10**). To prevent the formation of copper-ammonia

complexes, pH conditions are modified by reducing the inoculation proportion, referred to also as the second step. As a result, the copper immobilization efficiency remains very high when even subjected to higher $Cu(NO_3)_2$ concentrations. The use of the two-step biomineralization to secure the urease activity and also to modify pH conditions is considered of great necessity while applying the MICP technology to remedy copper-rich water bodies.

Conclusion

The proposed two-step biomineralization approach to secure the urease activity and also to modify pH conditions to prevent the copper-ammonia complexes formation was applied to copper immobilization. Based on the results and discussion, some main conclusions can be drawn as follows:

(1) The copper immobilization efficiency way below 10% for the bacterial inoculation proportion = 1:1 is attained and still holds true even when $Cu(NO_3)_2$ concentration is reduced to 5 mM. Although higher inoculation proportions can improve the resistance of the ureolytic bacteria against Cu^{2+} toxicity, their use is accompanied by discharging more OH^-, turning

surrounding environments into alkaline conditions and promoting the formation of copper-ammonia complexes. For this reason, the potential of Cu^{2+} migration is raised, causing an inability of securing the copper immobilization efficiency.

(2) 20–50 mM $Cu(NO_3)_2$ can badly depress the ureolytic bacteria and then reduces the degree of urea hydrolysis. The lower the degree of urea hydrolysis, the lesser the carbonate precipitated, and the lower the copper immobilization efficiency. The lack of CO_3^{2-}, induced by the reduction in the degree of urea hydrolysis, is considered to be the main cause leading to the copper immobilization efficiency way below 10% when subjected to 20–50 mM $Cu(NO_3)_2$.

(3) Under pH in a 4–6 range (in most cases), the copper immobilization efficiency is attained through azurite precipitation. The copper immobilization efficiency drops to zero under pH below 4 due to Cu^{2+} migration and diffusion. Under pH surrounding 9, the copper-ammonia complexes reduce the copper immobilization efficiency to zero. In case pH falls within a 7–9 range (in most cases), the copper immobilization efficiency is attained through malachite precipitation. The findings shed light on the necessity of securing the urease activity and modifying pH conditions while applying the MICP technology to remedy copper-rich water bodies.

Data availability statement

The original contributions presented in this study are included in the article/supplementary material, further inquiries can be directed to the corresponding author/s.

Author contributions

Funding

Conflict of interest

The authors declare that the research was conducted in the absence of any commercial or financial relationships that could be construed as a potential conflict of interest.

Publisher's note

All claims expressed in this article are solely those of the authors and do not necessarily represent those of their affiliated organizations, or those of the publisher, the editors and the reviewers. Any product that may be evaluated in this article, or claim that may be made by its manufacturer, is not guaranteed or endorsed by the publisher.

References

Achal, V., Pan, X. L., Fu, Q. L., and Zhang, D. Y. (2012a). Biomineralization based remediation of As (III) contaminated soil by Sporosarcina ginsengisoli. *J. Hazard. Mater.* 20, 178–184. doi: 10.1016/j.jhazmat.2011.11.067

Achal, V., Pan, X. L., Zhang, D. Y., and Fu, Q. L. (2012b). Bioremediation of Pb-Contaminated Soil Based on Microbially Induced Calcite Precipitation. *J. Microbiol. Biotechnol.* 22, 244–247. doi: 10.4014/jmb.1108.08033

Achal, V., Pan, X. L., and Zhang, D. Y. (2011). Remediation of copper-contaminated soil by Kocuria flava CR1, based on microbially induced calcite precipitation. *Ecol. Eng.* 37, 1601–1605. doi: 10.1016/j.ecoleng.2011.06.008

Ali, A., Li, M., Su, J., Li, Y., Wang, Z., Bai, Y., et al. (2022). Brevundimonas diminuta isolated from mines polluted soil immobilized cadmium (Cd^{2+}) and zinc (Zn^{2+}) through calcium carbonate precipitation: Microscopic and spectroscopic investigations. *Sci. Total Environ.* 813:152668. doi: 10.1016/j.scitotenv.2021.152668

Bai, B., Rao, D., Chang, T., and Guo, Z. (2019). A nonlinear attachment-detachment model with adsorption hysteresis for suspension-colloidal transport in porous media. *J. Hydrol.* 578:124080. doi: 10.1016/j.jhydrol.2019.124080

Bai, X. D., Cheng, W. C., and Li, G. (2021b). A comparative study of different machine learning algorithms in predicting EPB shield behaviour: A case study at the Xi'an metro, China. *Acta Geotech.* 16, 4061–4080. doi: 10.1007/s11440-021-01383-7

Bai, X. D., Cheng, W. C., Sheil, B. B., and Li, G. (2021c). Pipejacking clogging detection in soft alluvial deposits using machine learning algorithms. *Tunn. Undergr. Space Technol.* 113, 103908. doi: 10.1016/j.tust.2021.103908

Bai, B., Nie, Q., Zhang, Y., Wang, X., and Hu, W. (2021a). Cotransport of heavy metals and SiO_2 particles at different temperatures by seepage. *J. Hydrol.* 597:125771. doi: 10.1016/j.jhydrol.2020.125771

Casas, C. C., Graf, A., Brüggemann, N., Schaschke, C. J., and Jorat, M. E. (2020). Dolerite Fines Used as a Calcium Source for Microbially Induced Calcite Precipitation Reduce the Environmental Carbon Cost in Sandy Soil. *Front. Microbiol.* 2020:557119. doi: 10.3389/fmicb.2020.557119

Chen, L., Zhou, M., Wang, J., Zhang, Z., Duan, C., Wang, X., et al. (2022a). A global meta-analysis of heavy metal(loid)s pollution in soils near copper mines: Evaluation of pollution level and probabilistic health risks. *Sci. Total Environ.* 835:155441. doi: 10.1016/j.scitotenv.2022.155441

Chen, L., Beiyuan, J., Hu, W., Zhang, Z., Duan, C., Cui, Q., et al. (2022b). Phytoremediation of potentially toxic elements (PTEs) contaminated soils using alfalfa (*Medicago sativa L.*): A comprehensive review. *Chemosphere* 293:133577. doi: 10.1016/j.chemosphere.2022.133577

Chen, L., Wang, J. Z., Beiyuan, J. Z., Guo, X. T., Wu, H., and Fang, L. C. (2022c). Environmental and health risk assessment of potentially toxic trace elements in soils near uranium (U) mines: A global meta-analysis. *Sci. Total Environ.* 816:151556. doi: 10.1016/j.scitotenv.2021.151556

Chen, X. Y., and Achal, V. (2019). Biostimulation of carbonate precipitation process in soil for copper immobilization. *J. Hazard. Mater.* 368, 705–713. doi: 10.1016/j.jhazmat.2019.01.108

Chen, Z., Pan, X. H., Chen, H., Guan, X., and Lin, Z. (2016). Biomineralization of Pb(II) into Pb- hydroxyapatite induced by Bacillus cereus 12-2 isolated from Lead-Zinc mine tailings. *J. Hazard. Mater.* 301, 531–537. doi: 10.1016/j.jhazmat.2015.09.023

Cui, M. J., Lai, H. J., Hoang, T., and Chu, J. (2021). One-phase-low-pH enzyme induced carbonate precipitation (EICP) method for soil improvement. *Acta Geotech.* 16, 481–489. doi: 10.1007/s11440-020-01043-2

Cui, M. J., Teng, A., Chu, J., and Cao, B. (2022). A quantitative, high-throughput urease activity assay for comparison and rapid screening of ureolytic bacteria. *Environ. Res.* 208:112738. doi: 10.1016/j.envres.2022.112738

Duarte-Nass, C., Rebolledo, K., Valenzuela, T., Kopp, M., Jeison, D., Rivas, M., et al. (2020). Application of microbe-induced carbonate precipitation for copper removal from copper-enriched waters: Challenges to future industrial application. *J. Environ. Manag.* 256:109938. doi: 10.1016/j.jenvman.2019.109938

Elalfy, M., Abomosallam, M., Elhadidy, M. G., and Sleem, F. (2021). Copper and copper containing pesticide as copper oxychloride toxicity and its adverse effects on animal and human health. *Med. Res. Chron.* 8, 89–98. doi: 10.26838/MEDRECH.2021.8.2.486

Facchin, V., Cavinato, C., Fatone, F., Pavan, P., Cecchi, F., and Bolzonella, D. (2013). Effect of trace element supplementation on the mesophilic anaerobic digestion of foodwaste in batch trials: The influence of inoculum origin. *Biochem. Eng. J.* 70, 71–77. doi: 10.1016/j.bej.2012.10.004

Ferris, F. G., Phoenix, V., Fujita, Y., and Smith, R. W. (2004). Kinetics of calcite precipitation induced by ureolytic bacteria at 10 to 20°C in artificial groundwater. *Geochim. Cosmochim. Acta.* 67, 1701–1722. doi: 10.1016/S0016-7037(03)00503-9

Fu, F. L., and Wang, Q. (2011). Removal of heavy metal ions from wastewaters: A review. *J. Environ. Manag.* 92, 407–418. doi: 10.1016/j.jenvman.2010.11.011

Guo, H. R., Ouyang, Y. J., Wang, J. Q., Cui, H. M., Deng, H. D., Zhong, X. Y., et al. (2021). Cu-induced spermatogenesis disease is related to oxidative stress-mediated germ cell apoptosis and DNA damage. *J. Hazard. Mater.* 416:125903. doi: 10.1016/j.jhazmat.2021.125903

Hu, W., Cheng, W. C., and Wen, S. (2022a). Investigating the effect of degree of compaction, initial water content, and electric field intensity on electrokinetic remediation of an artificially Cu- and Pb-contaminated loess. *Acta Geotech.* doi: 10.1007/s11440-022-01602-9 [Epub ahead of print].

Hu, W., Cheng, W. C., Wang, L., and Xue, Z. F. (2022b). Micro-structural characteristics deterioration of intact loess under acid and saline solutions and resultant macro-mechanical properties. *Soil Tillage Res.* 220:105382. doi: 10.1016/j.still.2022.105382

Hu, W., Cheng, W. C., Wen, S., and Rahman, M. M. (2021a). Effects of chemical contamination on microscale structural characteristics of intact loess and resultant macroscale mechanical properties. *CATENA* 203:105361. doi: 10.1016/j.catena.2021.105361

Hu, W., Cheng, W. C., Wen, S., and Yuan, K. (2021b). Revealing enhancement and degradation mechanisms affecting calcite precipitation in EICP process. *Front. Bioeng. Biotechnol.* 9:750258. doi: 10.3389/fbioe.2021.750258

Jiang, N.-J., Liu, R., Du, Y.-J., and Bi, Y.-Z. (2019). Microbial induced carbonate precipitation for immobilizing Pb contaminants: Toxic effects on bacterial activity and immobilization efficiency. *Sci. Total Environ.* 672, 722–731. doi: 10.1016/j.scitotenv.2019.03.294

Jiang, N.-J., and Soga, K. (2019). Erosional Behavior of Gravel-Sand Mixtures Stabilized by Microbial Induced Calcite Precipitation (MICP). *Soils Found.* 59, 699–709. doi: 10.1016/j.sandf.2019.02.003

Kang, C. H., Oh, S. J., Shin, Y., Han, S. H., Nam, I. H., and So, J. S. (2015). Bioremediation of lead by ureolytic bacteria isolated from soil at abandoned metal mines in South Korea. *Ecol. Eng.* 74, 402–407. doi: 10.1016/j.ecoleng.2014.10.009

Kim, Y., Kwon, S., and Roh, Y. (2021). Effect of Divalent Cations (Cu, Zn, Pb, Cd, and Sr) on Microbially Induced Calcium Carbonate Precipitation and Mineralogical Properties. *Front. Microbiol.* 2021:646748. doi: 10.3389/fmicb.2021.646748

Krajewska, B. (2008). Mono- (Ag, Hg) and di- (Cu, Hg) valent metal ions effects on the activity of jack bean urease. Probing the modes of metal binding to the enzyme. *J. Enzyme Inhib. Med. Chem.* 23, 535–542. doi: 10.1093/emboj/cdg128

Lai, Y., Yu, J., Liu, S., and Dong, B. (2020). Experimental study to improve the mechanical properties of iron tailings sand by using MICP at low pH. *Constr. Build. Mater.* 273:121729. doi: 10.1016/j.conbuildmat.2020.121729

Li, M., Cheng, X. H., and Guo, H. X. (2013). Heavy metal removal by biomineralization of urease producing bacteria isolated from soil. *Int. Biodeterior. Biodegradation* 76, 81–85. doi: 10.1016/j.ibiod.2012.06.016

Li, Q., Wang, Y. H., Li, Y. C., Li, L. F., Tang, M. D., Hu, W. F., et al. (2022). Speciation of heavy metals in soils and their immobilization at micro-scale interfaces among diverse soil components. *Sci. Total Environ.* 825:153862. doi: 10.1016/j.scitotenv.2022.153862

Li, W. L., Fishman, A., and Achal, V. (2021). Ureolytic bacteria from electronic waste area, their biological robustness against potentially toxic elements and underlying mechanisms. *J. Environ. Manag.* 289:112517. doi: 10.1016/j.jenvman.2021.112517

Liu, F., Zhou, K. G., Chen, Q. Z., Wang, A. H., and Chen, W. (2018). Application of magnetic ferrite nanoparticles for removal of Cu (II) from copper-ammonia wastewater. *J. Alloys Compd.* 773:240. doi: 10.1016/j.jallcom.2018.09.240

Liu, K. W., Jiang, N.-J., Qin, J. D., Wang, Y. J., Tang, C. S., and Han, X. L. (2021). An experimental study of mitigating coastal sand dune erosion by microbial- and enzymatic-induced carbonate precipitation. *Acta Geotech.* 16, 467–480. doi: 10.1007/s11440-020-01046-z

Liu, P., Hu, W. Y., Tian, K., Huang, B., Zhao, Y. C., Wang, X. K., et al. (2020). Accumulation and ecological risk of heavy metals in soils along the coastal areas of the Bohai Sea and the Yellow Sea: A comparative study of China and South Korea. *Environ. Int.* 137:105519. doi: 10.1016/j.envint.2020.105519

Mugwar, A. J., and Harbottle, M. J. (2016). Toxicity effects on metal sequestration by microbially-induced carbonate precipitation. *J. Hazard Mater.* 314, 237–248. doi: 10.1016/j.jhazmat.2016.04.039

Mujah, D., Shahin, M. A., Cheng, L., and Karrech, A. (2021). Experimental and Analytical Study on Geomechanical Behavior of Biocemented Sand. *Int. J. Geomech.* 21:0002105. doi: 10.1061/(ASCE)GM.1943-5622.0002105

Qdais, H. A., and Moussa, H. (2004). Removal of heavy metals from wastewater by membrane processes: A comparative study. *Desalination* 164, 105–110. doi: 10.1016/S0011-9164(04)00169-9

Qiao, S., Zeng, G., Wang, X., Dai, C., Sheng, M., Chen, Q., et al. (2021). Multiple heavy metals immobilization based on microbially induced carbonate precipitation by ureolytic bacteria and the precipitation patterns exploration. *Chemosphere* 274:129661. doi: 10.1016/j.chemosphere.2021.129661

Rahman, M. M., Hora, R. N., Ahenkorah, I., Beecham, S., Karim, M. R., and Iqbal, A. (2020). State-of-the-art review of microbial-induced calcite precipitation and its sustainability in engineering applications. *Sustainability* 12:6281. doi: 10.3390/su12156281

Schwantes-Cezario, N., Camargo, G., Couto, L., Porto, M. F., and Toralles, B. M. (2020). Mortars with the addition of bacterial spores: Evaluation of porosity using different test methods. *J. Build. Eng.* 30:101235. doi: 10.1016/j.jobe.2020.101235

Schwantes-Cezario, N., Medeiros, L. P., Oliveira, A. D., Nakazato, G., Renata, K., and Toralles, B. M. (2017). Bioprecipitation of calcium carbonate induced by bacillus subtilis isolated in brazil. *Int. Biodeterior. Biodegradation* 123, 200–205. doi: 10.1016/j.ibiod.2017.06.021

Seplveda, S., Duarte-Nass, C., Rivas, M., Azcar, L., Ramrez, A., Toledo-Alarcn, J., et al. (2021). Testing the Capacity of Staphylococcus equorum for Calcium and Copper Removal through MICP Process. *Minerals* 11:905. doi: 10.3390/min11080905

Song, B., Zeng, G. M., Gong, J. L., Liang, J., Xu, P., Liu, Z. F., et al. (2017). Evaluation methods for assessing effectiveness of in situ remediation of soil and sediment contaminated with organic pollutants and heavy metals. *Environ. Int.* 105, 43–55. doi: 10.1016/j.envint.2017.05.001

Tarach, K. A., Jabońska, M., Pyra, K., Liebau, M., and Góra-Marek, K. (2021). Effect of zeolite topology on NH_3-SCR activity and stability of Cu-exchanged zeolites. *Appl. Catal. B* 2021:119752. doi: 10.1016/j.apcatb.2020.119752

Torres-Aravena, A. E., Duarte-Nass, C., Azcar, L., Mella-Herrera, R., Rivas, M., and Jeison, D. (2018). Can Microbially Induced Calcite Precipitation (MICP) through a Ureolytic Pathway Be Successfully Applied for Removing Heavy Metals from Wastewaters? *Crystals* 8:438. doi: 10.3390/cryst8110438

Wang, L., Cheng, W. C., and Xue, Z. F. (2022b). Investigating microscale structural characteristics and resultant macroscale mechanical properties of loess exposed to alkaline and saline environments. *Bull. Eng. Geol. Environ.* 81:146. doi: 10.1007/s10064-022-02640-z

Wang, H., Yun, H., Ma, X. D., Li, M. H., Qi, M. Y., Wang, L., et al. (2022a). Bioelectrochemical catabolism of triclocarban through the cascade acclimation of triclocarban-hydrolyzing and chloroanilines-oxidizing microbial communities. *Environ. Res.* 210:112880. doi: 10.1016/j.envres.2022.112880

Wang, Z., Su, J. F., Ali, A., Sun, Y., Li, Y. F., Wang, W. S., et al. (2022e). Enhanced removal of fluoride, nitrate, and calcium using self-assembled fungus-flexible fiber composite microspheres combined with microbially induced calcium precipitation. *Chemosphere* 302:134848. doi: 10.1016/j.chemosphere.2022.134848

Wang, Z., Su, J. F., Ali, A., Yang, W. S., Zhang, R. J., Li, Y. F., et al. (2022f). Chitosan and carboxymethyl chitosan mimic biomineralization and promote microbially induced calcium precipitation. *Carbohydr. Polym.* 287:119335. doi: 10.1016/j.carbpol.2022.119335

Wang, L., Cheng, W. C., and Xue, Z. F. (2022c). The effect of calcium source on Pb and Cu remediation using enzyme-induced carbonate precipitation. *Front. Bioeng. Biotechnol.* 10:849631. doi: 10.3389/fbioe.2022.849631

Wang, L., Cheng, W. C., Xue, Z. F., and Hu, W. (2022d). Effects of the urease concentration and calcium source on enzyme-induced carbonate precipitation for lead remediation. *Front. Chem.* 10:892090. doi: 10.3389/fchem.2022.892090

Wei, S. H., Zhou, Q. X., and Wang, X. (2005). Identification of weed plants excluding the uptake of heavy metals. *Environ. Int.* 31, 829–834. doi: 10.1016/j.envint.2005.05.045

Whiffin, V. S., van Paassen, L. A., and Harkes, M. P. (2007). Microbial carbonate precipitation as a soil improvement technique. *Geomicrobiol. J.* 24, 417–423. doi: 10.1080/01490450701436505

Xiao, Y., Wang, Y., Wang, S., Matthew Evans, T., Stuedlein, A. W., Chu, J., et al. (2021). Homogeneity and mechanical behaviors of sands improved by a temperature-controlled one-phase MICP method. *Acta Geotech.* 16, 1417–1427. doi: 10.1007/s11440-020-01122-4

Xue, Z. F., Cheng, W. C., Wang, L., and Hu, W. L. (2022a). Effects of bacterial inoculation and calcium source on microbial-induced carbonate precipitation for lead remediation. *J. Hazard. Mater.* 426:128090. doi: 10.1016/j.jhazmat.2021.128090

Xue, Z. F., Cheng, W. C., Wang, L., and Song, G. Y. (2021). Improvement of the shearing behaviour of loess using recycled straw fiber reinforcement. *KSCE J. Civ. Eng.* 25, 3319–3335. doi: 10.1007/s12205-021-2263-3

Xue, Z. F., Cheng, W. C., Wang, L., Qin, P., and Zhang, B. (2022c). Revealing degradation and enhancement mechanisms affecting copper (Cu) immobilization using microbial-induced carbonate precipitation (MICP). *J. Environ. Chem. Eng.* 10:108479. doi: 10.1016/j.jece.2022.108479

Xue, Z. F., Cheng, W. C., Wang, L., and Wen, S. J. (2022b). Effects of Bacterial Culture and Calcium Source Addition on Lead and Copper Remediation Using Bioinspired Calcium Carbonate Precipitation. *Front. Bioeng. Biotechnol.* 10:889717. doi: 10.3389/fbioe.2022.889717

Yang, Y., Chu, J., Liu, H., and Cheng, L. (2022). Improvement of uniformity of biocemented sand column using CH3COOH-buffered one-phase-low-pH injection method. *Acta Geotech.* 228. doi: 10.1007/s11440-022-01576-8

Ye, X. Y., Zheng, X. X., Zhang, D. Q., Niu, X. J., Fan, Y. M., Deng, W. D., et al. (2021). The efficient biomineralization and adsorption of cadmium (Cd^{2+}) using secretory organo-biominerals (SOBs) produced by screened Alcaligenes faecalis K2. *Environ. Res.* 2021:111330. doi: 10.1016/j.envres.2021.111330

You, S. Z., Hu, Y., Liu, X. C., and Wei, C. H. (2018). Synergetic removal of Pb(II) and dibutyl phthalate mixed pollutants on Bi_2O_3-TiO_2 composite photocatalyst under visible light. *Appl. Catal. B Environ.* 232, 288–298. doi: 10.1016/j.apcatb.2018.03.025

Yu, D. Y., Wang, J. R., Wang, Y. H., Du, X. L., Li, G. C., and Li, B. (2021). Identifying the Source of Heavy Metal Pollution and Apportionment in Agricultural Soils Impacted by Different Smelters in China by the Positive Matrix Factorization Model and the Pb Isotope Ratio Method. *Sustainability* 13:6526. doi: 10.3390/su13126526

Zaborska, W., Krajewska, B., and Olech, Z. (2004). Heavy Metal Ions Inhibition of Jack Bean Urease: Potential for Rapid Contaminant Probing. *J. Enzyme Inhib. Med. Chem.* 19, 65–69. doi: 10.1118/1.1624755

Zeng, C., Veenis, Y., Hall, C. A., Young, E. S., van der Star, W. R. L., Zheng, J. J., et al. (2021). Experimental and Numerical Analysis of a Field Trial Application of Microbially Induced Calcite Precipitation for Ground Stabilization. *J. Geotech. Geoenviron. Eng.* 147:05021003. doi: 10.1061/(ASCE)GT.1943-5606.0002545

Zhang, K. J., Xue, Y. W., Zhang, J. Q., and Hu, X. L. (2020). Removal of lead from acidic wastewater by bio-mineralized bacteria with pH self-regulation. *Chemosphere* 241:125041. doi: 10.1016/j.chemosphere.2019.125041